Global J. Environ. Sci. Manage. 6(1): 31-46, Winter 2020

Global Journal of Environmental Science and Management
(GJESM)

Homepage: https://www.gjesm.net/

ORIGINAL RESEARCH PAPER

Environmental sensitivity of flash flood hazard using geospatial techniques

H.T. Abdel Hamid[1,2,*], W. Wenlong[2], L. Qiaomin[2]

[1] *Department of Marine Pollution, National Institute of Oceanography and Fisheries, Alexandria, Egypt*

[2] *Ningxia Institute of Remote Sensing Surveying and Mapping, Yinchuan 750021 China*

ARTICLE INFO

Article History:
Received 28 March 2019
Revised 12 July 2019
Accepted 15 September 2019

Keywords:
Analytical Hierarchy Process (AHP)
Disaster
Flash Flood
Remote Sensing (RS)
Shuttle Radar Topography Mission-Digital Elevation Model (SRTM-DEM)

ABSTRACT

Flash flood has been increasing in the Khartoum area, Sudan due to geographical conditions and climatic change as heavy rainfall and high temperature, therefore the present work tried to estimate the sensitivity of flash flood. The present work proposes an advanced technique of flood sensitivity mapping using the method of analytical hierarchy process. Ten factors as elevation, slope, distance from the network, land use, density of the drainage, flow accumulation, surface roughness, stream power index, topographic wetness index and curvature of the topography were digitized and then contributed in the mapping of Flash flood. Remote sensing data were integrated with analytical hierarchy process to determine the flood sensitive area in Sudan. The model was applied and completed as the consistency ratio was mostly reasonable (< 0.1). Based on the proposed model, about 75.56 Km^2 (12.26 %), 156.14 Km^2 (25.33%), 169.89 Km^2 (27.56 %), 141.40 Km^2 (22.94 %) and 73.50 Km^2 (11.92 %); were classified as no susceptible, low susceptible, high susceptible, moderate susceptible and very highly susceptible to flooding. The present study showed a high variation in flood sensitivity due to climatic change and geographic condition. This index can be modified and applied in areas of the same characteristics of climatic conditions as one of the main recommendation in the study area. The study showed that poor infrastructure and lack of preparedness were the main causes of the disaster of flood in Sudan. This study merely demonstrated the critical analysis of geospatial mapping in proper mitigating, sustainable development and great monitoring the negative effects of flooding along the Khartoum region to reduce hazards of flood.

DOI: 10.22034/gjesm.2020.01.03

NUMBER OF REFERENCES	NUMBER OF FIGURES	NUMBER OF TABLES
33	6	7

*Corresponding Author:
Email: *hazem_ecology@yahoo.com*
Phone: +86136 29504606
Fax: +9513 957502

Note: Discussion period for this manuscript open until April 1, 2020 on GJESM website at the "Show Article.

INTRODUCTION

Flash Floods are considered as one of the most destructive actions of a sensitive nature. Humanity, agriculture and other damages may be occurred due to flash floods (Kowalzig, 2008). About 170 million people around the world annually are affected by the floods therefore; management of flood needs to be taken into considerations (Kazakis *et al*., 2015). Floods have been the most periodic disasters documented in the emergency events database (EM-DAT), followed by earthquakes, storms and droughts, indicating a strong need for early warning systems and disaster risk management. The low percentage for droughts listed in the EM-DAT is due to limited data availability (EM-DAT, 2018). Nowadays, disasters of floods are widely concerning and distributing in some areas of the Nile River Basin, especially in Egypt and Sudan. In Sudan, the Flash floods are flooded regularly from June to October every year, causing great disasters. It has caused a certain degree of harm to the agriculture sector and residents especially lower area of the Nile River. As a result of urban sprawl and development in the industry sector, studying the hazard of flash flood has become very important for sustainable development (Abd El-Hamid, 2016). Nowadays, many Sudanese cities witnessed unprecedented floods as a result of heavy rains in the country. Floods and heavy flooding swept through areas and cities which located in the north of Khartoum about 40 km, including Jelly city, Zakiab city and Tibnah-Kidro city. This flash flood led to the collapse of a large number of houses and residents to take refuge in high places, and some families were forced to take shelter and protect themselves in schools and other local building. Climate changes are the result of high temperature, precipitation, heavy rain and seasonal variations, therefore these changes are responsible for flood occurrence. Every year, floods in Sudan killing and injuring more than 140 people, damaging of thousands of homes and causing the deaths of herds of cattle. Ecosystem and environment may be affected negatively by some metrological parameters that increase the risk and pressure on the hydrological system causing severs prediction of flood in the urban area (Muneerudeen, 2017). Coulibaly (2008) said that flash flood may be developed after raising the surface water on the low land areas. People who are living in these low lands may be undergone the danger of flash flood, especially in urban and rural sites. Flash flood may be occurred by heavy rain, dam break or other anthropogenic activities. Narrow valleys produce quickly fluid water which rises rapidly to a substantial depth (NOAA/NWS, 2005). A strong link among total precipitation and rainfall during the season of the flood (Chi *et al*., 2019). Sulieman and Elagib (2012) stated that flood is the most popular natural hazard in Sudan causing severs destruction; therefore critical interest was applied from the decision-maker and the government. Because of the uncertainties, suddenness and regional characteristics of floods, it is difficult to realize the development of floods promptly, comprehensively grasp the progress of disasters, and accurately assess the loss of floods. Hazard degree (low, medium or high) was based on the water depth and velocity, while the risk degree was based on the vulnerability of an area. By combining maps with the current and planned urbanization extent, a decision can be made about the accepted level of risk. Thus, the protection to the vulnerable areas could be executed (Abdulrazzak *et al*., 2019). It is difficult to achieve by relying solely on communication and ground transportation. Modern applications of remote sensing technology, Geographic Information system (GIS), and new technologies such as numerical simulations and mathematical models, provide a new means for the investigation, calculation, simulation, analysis, evaluation and prevention of flood disasters. In the present study, anew chines satellite was applied for flood hazards. Technologies of remote sensing and GIS are important sources of data integration and decision making for sustainable development (Adinarayana and Krishna, 1996). Therefore, the application of remote sensing monitoring technology and other damage assessment studies for flood inundation is the basis for disaster prevention and mitigation work in in the Nile River floods. Analytic Hierarchy Process (AHP) is among the spatial multi-criteria analyses for assessing the area sensitive to flood risk. Prediction of flood hazard in any region requires some data of mining approaches (Harun *et al*., 2017). Geospatial mapping and simulation of flash flood in developing countries can minimize economic losses and increase the probability of environmental development. To preserve the loss of aquatic life and human death, remote sensing

technology was applied in the study area. The main objective of this present study is to assess the risk of the flash flood in Khartoum, Sudan. To achieve this objective, remote sensing and GIS techniques have been integrated using as a spatial index called AHP method ranking the factors according to its importance for evaluating the excessive risk and critical vulnerability. It can be updated and applied in other regions. This study has been carried out in in Khartoum area, Sudan in 2018.

MATERIAL AND METHODS

Site description

Sudan is located in the upper and middle regions of the Nile River; Sudan properly belongs to the savanna climate. The annual rate of rainfall precipitation in Sudan is approximately 175 mm. The levels of the White Nile water and the Blue Nile were reported at 17.14 meters (min) in Khartoum, high level of water resulting from heavy rain in Ethiopia. Heavy rains cause devastating floods in different regions of Sudan (Elhaja *et al.*, 2017). Usually, water starts promptly to rise in May, the water level gradually decreases, and the low water level is precisely from January to May. The terrain along the Nile in Sudan is relatively flat, and the drainage is slow. The Blue Nile and White Nile rivers meet in Sudan, and the water volume is greatly increased, which is more susceptible to flood disasters in the Nile. Fig. 1 shows the study area that is selected from the Qing Nile River Basin, 15 kilometers (km) south of Khartoum, and the capital of Sudan. The local coordinates typically ranged from Latitudes 32°35′00′′ E - 33°02′16′′ E and Longitudes 15°14′33′′ N to 15°35′ 45′′ N with an area of about 560 km^2 and an average river width of 1 km. The effective length of the Qing Nile River section is about 70 km.

Climatic conditions and factors

Climate change is one of the most important issues of concern to many countries of the world in all aspects of political and economic life. However, it tocks a long time in almost 20 years to prioritize the discussion. The study area is adequately characterized by savanna climate, with obvious dry and rainy seasons and measurable precipitation

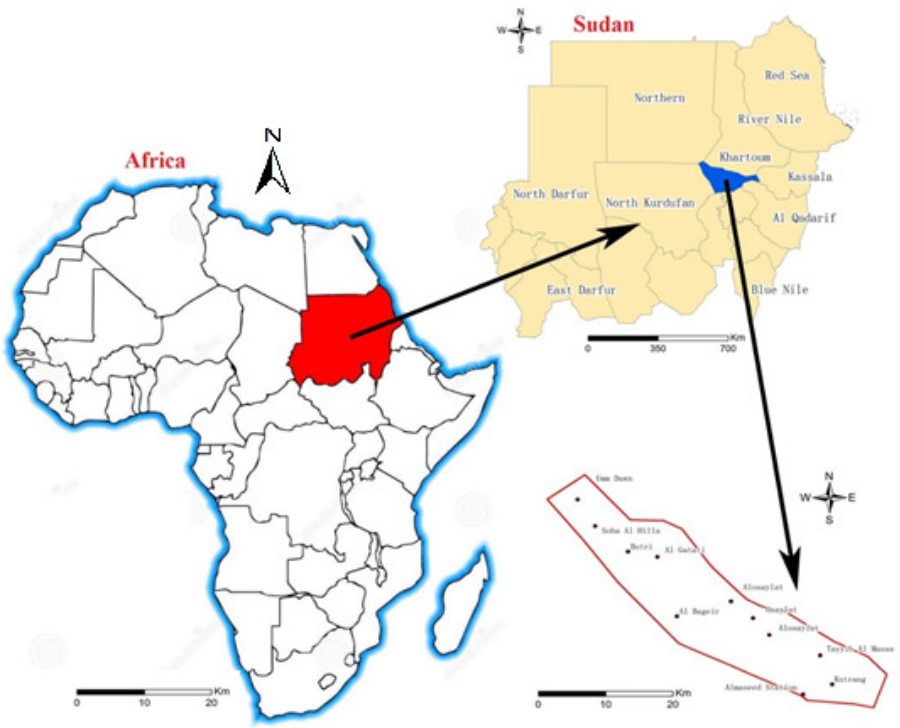

Fig. 1: Geographic location of the study area in Khartoum area, Sudan

during the rainy season. Fig. 2 shows the monthly temperature and rainfall of the study area. Temperature is very high in winter reach to 31°C in January, but sometimes cold at night, and the cold record is only 1°C; in spring. In July and August months, the temperature declines slightly, but it remains very high, and then between October and November, at the final of the monsoon, it increases slightly again (Anon, 2018). Although the floods take place commonly, the quantity of water and the tides differ significantly. Rainfall is one of the most factors of meteorological that leading to flooding in the study area (Dolman *et al.*, 1997). Poor and low aggregation of water resulted from a high temperature and low precipitation in arid regions, therefore a high probability of soil erosion and high

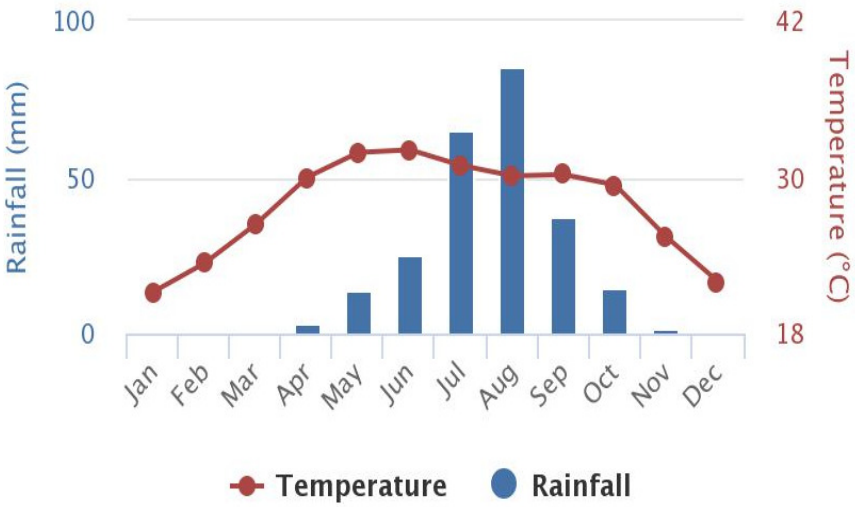

Fig. 2: Annual temperature and rainfall according to (Anon, 2018)

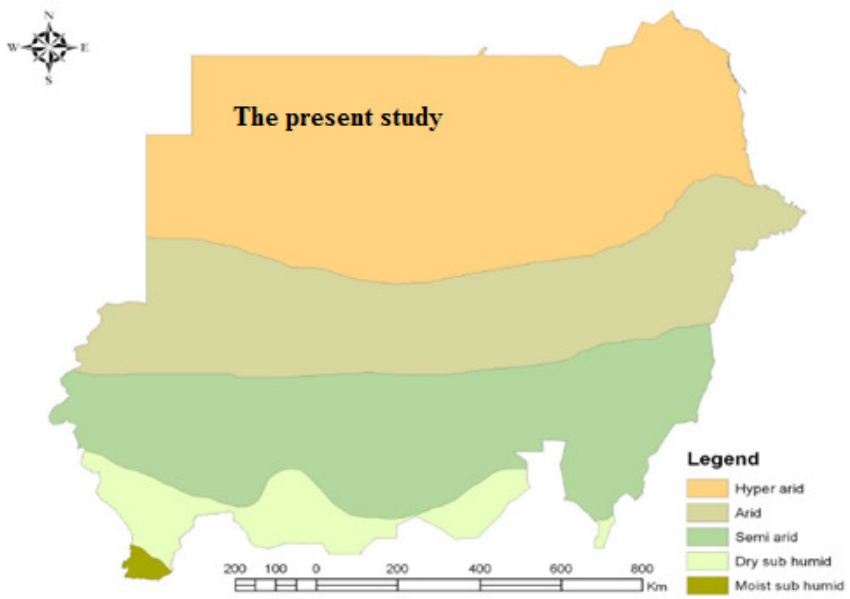

Fig. 3: Classification of climatic in zones of Sudan

Table 1: Characteristics of GF Series Satellites.

Satellite name	GF_1		GF_2
Spatial resolution	16m	2m / 8m	1m / 4m
Sensor	WFV	PMS	PMS
Width	800 Km	70 km	45 km

water level cause many problems to human life.

Climatic zones

Climatic zones of Sudan were shown in Fig. 3 representing the study area in the North of the Climatic zone. In the present study, the climate of Sudan may be classified into five zones according to temperature, rainfall, and abundant precipitation. It was classified into hyper-arid, arid, semi-arid, dry sub-humid and moist sub-humid. It was shown that large area of Sudan classified into hyper arid climate. The present study situated in the Northern part of Sudan as hyper arid climate.

Risk assessment

The Blue Nile and the Atbara River is the major factor causing severe risk in the study area. 80% of the Nile's rivers produced from the Ethiopian plateau. When the flood arrives, the farmland on both sides will be inundated. After the flood recedes, a thick layer of river mud will be left to form a fertile soil. The flood of the Nile River flows to Khartoum in June and reaches the highest water level in September. It is precise because of the seasonal changes in the water volume of the Blue Nile that the Nile River is typically regularly flooded and carries a lot of fertile soil and flows into the stream of the Nile River, causing regular flooding in the lower reaches of the Nile River and typically forming a fertile delta. The amount of water during the flood period mainly comes from the Blue Nile River, and the considerable amount of water during the dry season mainly comes from the White Nile.

Data set

Gaofen satellite (GF)

Gaofen (GF) is a sequence of Chinese civilian remote sensing satellites. In the present, 2 m resolution and a camera with 8 m resolution was used for mapping the hazard of the flash flood in Sudan. GF_2 satellite data was arbitrarily selected as the main data for mapping the hazard of the flood. Criteria of GF satellite are presented in Table 1. Satellite data was acquired in 2017 and 2018. According to the climate of the Arab countries, satellite data was merely selected during the period from vegetation and flood period. After acquiring the images, data preprocessing in the study area were applied. In the present study, FLASH method was applied. FLAASH method is an atmospheric correction that corrects mainly the wavelengths of visible near-infrared, and shortwave infrared information. The general FLAASH technique takes contribution from the radiance and gives an atmospheric surface reflectance image (Matthew *et al*., 2000).

Table 2: Accuracy data of SRTM DEM

Data	SRTM DEM
Minimum (min)	361.00900268555 (m)
Maximum (max)	406.78298950195 (m)
Standard deviation	7.6396240580124
Coordinates system	WGS_1984_UTM_Zone_36N
Angular unit (Degree)	0.0174532925199433°

Factors of flood susceptibility

Land cover classification

Susceptibility of the flood can mainly be influenced by land use and land cover changes. According to the field survey, topographic map of scale 1:25000 and remote sensing satellite data (GF) with 2-meter resolution, land use and land cover (LULC) was classified using Maximum likelihood supervised classification as the most accurate method in this present study to instantly detect different features. It makes use of a discriminant function to assign pixel to the class with the highest likelihood. In the present study, eight classes were extracted: transportation facilities, bare lands, urban, irrigated agriculture lands, rain agriculture lands, water bodies, forest lands, and agriculture lands. Detection and mapping of flood hazard are depending on some environmental factors that vary from one area to another. Many complex factors affecting flood mapping in the urban regions as constructions, roads, culverts, streams, tunnels, and underground structures (Hapuarachchi *et al*., 2011).

Digital elevation model

Digital elevation model (DEM) is representing the accurate earth surface topography. It is a vital tool in the hydrological models. DEM is responsible for extracting some factors associated with topographic conditions as slope, aspect, flow, fill, watershed, stream link and other hydrological parameters that effect on mapping flood in any region. (Kia *et al*., 2012). SRTM DEM (Shuttle Radar Topography Mission) gives accurate data which are vital in many environmental changes as hydrologic management and flood hazards. Digital Elevation Models are data files that contain the elevation of the terrain over a specified area, usually at a fixed grid interval over the surface of the earth. It composed of some layers of considerable elevations in relation to a datum, and then data have been corrected through a geographic coordinate system (Forkuo, 2010). In the study, The SRTM DEM with 4 m spatial resolution was used as the basis of slope, elevation, and aspect. The criteria of the Dem are shown in Table 2. From DEM map, elevation map was extracted as the most important factor of flood mapping.

Surface slope and aspect

The slope is one of the most effective factors in floods simulation and mapping. The hazard of flash flood increase as the slope increase causing damage to surrounding regions. The aspect factor affects the occurrence of natural phenomena of the earth surface as it is contributed to climatic factors as the direction of precipitation and the amount of sunshine. The slope is depending on the nature of earth surface (Forkuo, 2010).

Surface roughness (SR)

Surface roughness is the most significant variable in simulating and detecting flash flood simulation and analysis. Low surface roughness cause little penetration of water in the soil pores, therefore the damage reduced under high surface roughness (Kia *et al*., 2012).

Curvature topographic (CT)

Curvature is one of the most important factors of water velocity and its penetration in the earth surface through different sizes of soil (Cao *et al*., 2016). It ranges from one as the low probability to two as the high probability of flood. For the perfect illustration of flow velocity, it is useful to contain curvature as it funds the projection of the water depth (Horritt, 2000). Erosion is one of the major secondary impacts.

Topographic wetness index (TWI)

TWI was proposed by Beven and Kirkby (1979). It was used clearly to detect the topography effects on hydrological processes. Equilibrium of watershed also achieved by TWI between flow water accumulation and drainage in different scales of regions. Otherwise, it defines the trend of saturation for any site at the earth surface and its contributing area and local slope properties. It can be computed by Eq. 1.

$$\mathrm{TWI} = \ln\left(\frac{A_S}{tan\,\beta}\right) \quad (1)$$

Where, *As* characterizes the cumulative upslope in point of the region and tan β indicates the slope angle at the pour-point.

Stream power index (SPI)

The SPI is an indicator of stream erosion at a given point on the earth surface. The increasing value of SPI resulted from a high slope and high flow rate of water in a given area. Also, the amount of water contributed to the upward slope and the water flow rate increase, causing a high rate of SPI value. It can be assumed by Eq. 2.

$$\mathrm{SPI} = A_S tan\,\beta \quad (2)$$

Where, A_S indicates the definite catchment area, and β denotes the slope gradient.

Drainage density (Dd)

As higher drainage density, as the higher sensitivity to flooding in low land area. Kumar *et al*. (2007) showed that higher the flow of water the greater drainage density paralleled to the areas with low drainage density. Thus, the mapping of flood hazard associated with the drainage density, which is a serious variable for runoff production (Mahmoud and Gan, 2018) as shown in Eq. 3.

$$Dd = \frac{\Sigma\, \mathrm{l}}{\mathrm{A}} \quad (3)$$

Where, L is the total length of the streams and A is the area.

Distance to river

To protect the surrounding area and agriculture from flood hazard, the distance to river is very important. Distance to the river is a vital in the level of flood sensitivity in the study area. Generally, the area near to the point of the river is more vulnerable to flooding.

Flow accumulation

According to Kazakis *et al.* (2015), flow accumulation considered as one of the main important parameters in the mapping of the flood. High flow accumulation commonly leads to higher flood vulnerability**.** The runoff of flow in any zone is depending on the surrounding pixel (Mahmoud and Gan, 2018)**.** In the present study, flow accumulation, flow direction, aspects and other hydrological parameters resulting from DEM.

Analytical hierarchy process (AHP)

In the present study, AHP is a multi-criteria decision-making approach which was introduced by Mastin (2009). The AHP is a decision support model for solving complex decision problems, uses a multi-level hierarchical structure of aims, conditions, sub-criteria and changes. These factors were selected based on different studies with similar characteristics. Using the relative comparison matrix, a comparison was made between the factors influencing the probability of flooding in the study area. This matrix is subjected to the opposite rows of each component and its importance with the other factor. For example, the elevation is of great importance than slope. Therefore, elevation takes the first important factor and slope the second factor (Table 3). The work of the matrix compared to a uniform even where diagonal elements are equal to 1, as computed in Eq. 4.

$$Pij=\begin{pmatrix} p_{11} & p_{12} & p_{1n} \\ p_{21} & p_{22} & p_{2n} \\ p_{n1} & p_{n2} & p_{nn} \end{pmatrix} \quad (4)$$

Where, p is the probability of each factor in the matrix to n: number of factors. Through the weighted average method, the comparative materials of the even pairs are calculated to calculate the standard comparison matrix of the pair (Table 4). If the consistency ratio (CR) value is less than 0.1, the final map of suitability is ready for comparison and interpretation and the data is acceptable. On the other hand; if the value is greater than 0.1, the comparison matrix indicates inconsistency and the results are readjusted according to Saaty (1977). Table 5 indicates that the CR values for some components are lower than 0.10, which indicates the preferences made in this study are highly consistent, on the other hand some of these factors are higher than 0.1 as limitation of this study. It can

Table 3: Comparison matrix and relative score of each parameter

Parameter	Elevation	Slope	Distance	Drainage	Flow	LULC	SPI	TWI	Curvature
Elevation	1	2	3	4	5	6	7	8	9
Slope	½	1	2	3	4	5	6	7	8
Distance	1/3	½	1	2	3	4	5	6	7
Drainage	¼	1/3	½	1	2	3	4	5	6
Flow	1/5	¼	1/3	½	1	2	3	4	5
LULC	1/6	1/5	¼	1/3	½	1	2	3	4
SPI	1/7	1/6	1/5	¼	1/3	½	1	2	3
TWI	1/8	1/7	1/6	1/5	¼	1/3	½	1	2
Curvature	1/9	1/8	1/7	1/6	1/5	1/4	1/3	1/2	1

Table 4: Normalized weight values in the standardized pairwise comparison matrix

Parameter	TWI	SPI	Slope	LULC	Flow direction	Curvature	DEM
TWI	0	-	-	-	-	-	-
SPI	-3.69	0	-	-	-	-	-
Slope	-0.54	-1.88	0	-	-	-	-
LULC	-3.55	-3.13	-1.33	0	-	-	-
Flow direction	0.61	-3.47	-1.85	-7.12	0	-	-
Curvature	-2.43	-2.5	-0.88	-4.13	-3.01	0	-
Elevation	-0.59	-1.56	-0.25	-0.56	-3.17	-4.16	0
Distance	4	-1.29	-2.12	-0.89	-1.82	-2.8	-1.8

Table 5: Classification of Flood susceptibility Index (FSI)

Factor	Type/ degree	CR
LULC	Bare and Water Wood and Grass Agriculture and Cultivated Transportation Urban	0.05
Slope (%)	0-0.1349 0.1349-0.1436 0.1436- 0.278 0.278-2.37 2.37-34.96	0.0299
Surface Roughness	0-0.45 0.45-0.49 0.49-0.502 0.502-0.547 0.547-1	-
Elevation (m)	361.02-374.29 374.29-381.83 381.38-387.39 387.39-392.42 392.42-406.78	0.1719
Flow Accumulation(m)	0-0.899 0.899-1.358 1.358-2.258 2.258-4. 02 4.02-7.49	0.0942
SPI	-1.42 to -0.173 -0.173 to -0.059 -0.059 - 0.021 0.021- 0.0706 0.0706 - 2.723	0.0267
TWI	-6907.7 to -1725.7 -1725.72 – 789.08 789.08 – 1855.9 1855.9 – 3761.13 3761.13 – 12524.8	0.0204
Curvature	-7347 to -50.057 -50.057 to -25.56 -25.56 to -0.061 -0.061 to 26.86 26.86 – 52.486	0.0933
Distance	0-5600 5600-11200 11200-16800 16800-22400 22400-28000	0.2057
Drainage density	1-1.8 1.8-2.6 2.6-3.4 3.4-4.2 4.2-5	0.0756

be computed using Eqs. 5 and 6.

$$CR = \frac{CI}{RI} \quad (5)$$

Where random index (RI) gives the randomly produced mean consistency index and consistency index (CI) is calculated as Eq. 6.

showed that
drainage den (6)

Where λ_{max} shows the highest eigenvalue of the matrix and "n" gives the accurate sequence of the matrix.

For mapping the hazard of flood in the study area, combination of all factors and their importance according to the weighing value using environments of ArcGIS. FSI is calculated using Eq. 7.

$$FSI = \sum_{i=1}^{n} w_i * r_i \quad (7)$$

Where FSI is the flood susceptibility index, W_i is the weight value of every variable; R_i is the weight value

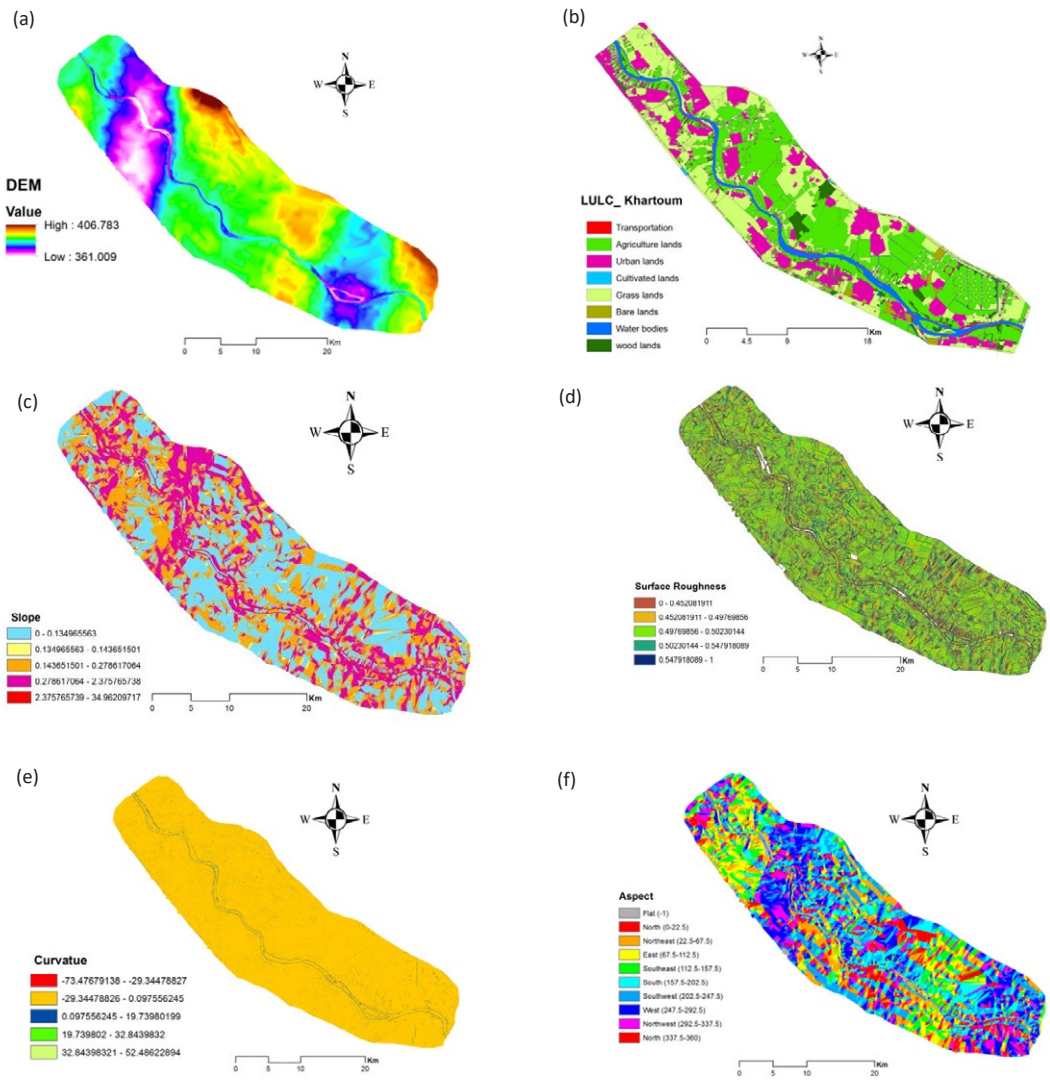

Fig. 4(a): Factors of flood sensitivity: a) DEM; b) LULC; c) Gradient slope; d) Surface roughness; e) Curvature and (F): Aspect of the study area

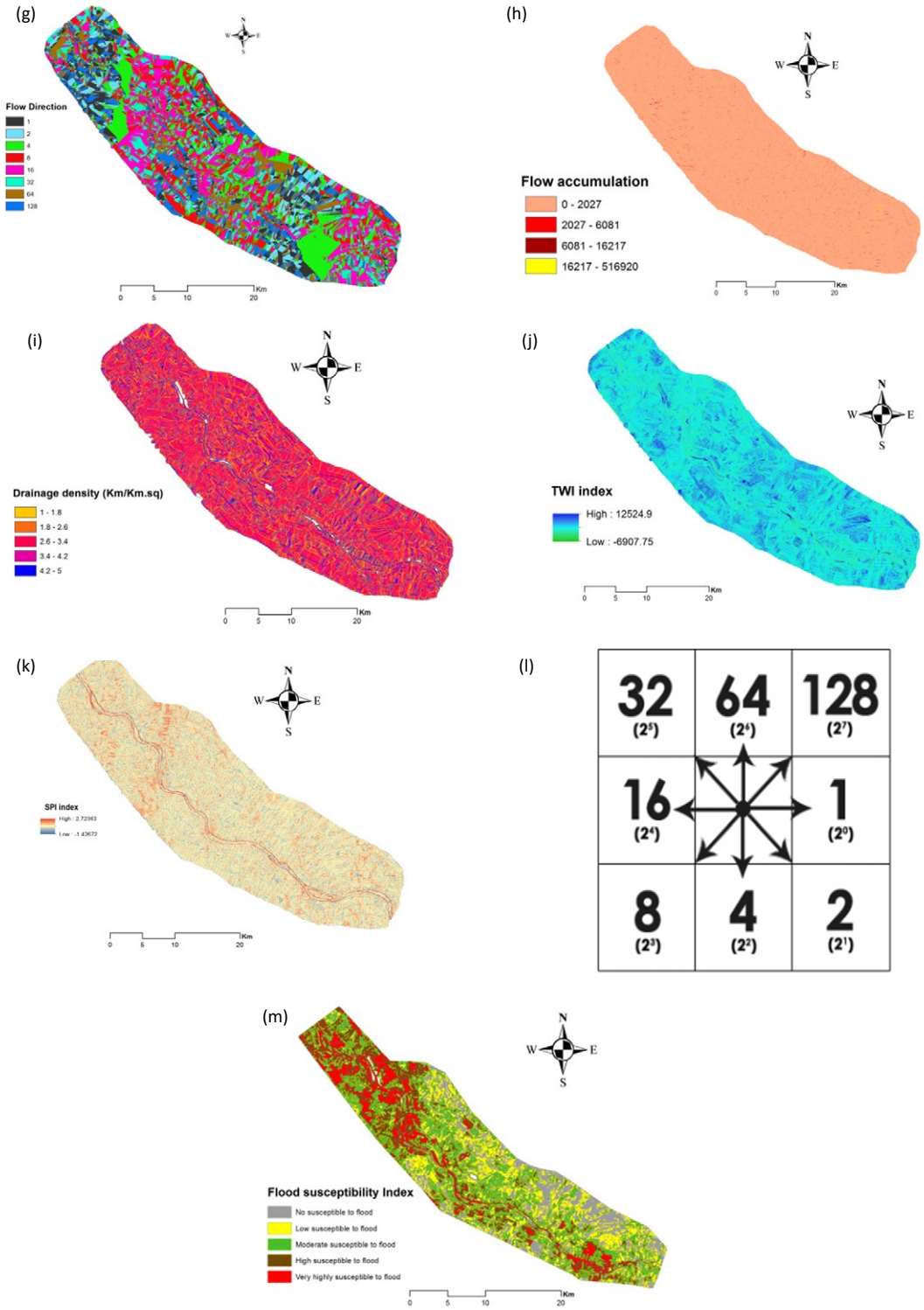

Fig. 4(b): Factors of flood sensitivity and final map of sensitivity: g) Flow direction; h) Flow accumulation; i) Drainage density; j) TWI; k) SPI; i) pour-point model diagram and (m): FSI of the study area

Table 6: Land use and land cover change (LULC) of the study area

Class name	Class name	Area (km²)	Percentage (%)
Class 1	Transportation lands	4.330805	0.71
Class 2	Bare lands	9.498543	1.56
Class 3	Construction (Urban) lands	115.889027	19.07
Class 4	Irrigated agriculture lands (Cultivated)	0.485472	0.08
Class 5	Rain agriculture lands (Grasslands)	194.906534	32.07
Class 6	Water bodies	32.624513	5.37
Class 7	Woodlands	20.916534	3.44
Class 8	Agriculture lands	229.114881	37.70

of every class of different factors, n is the number of factors. In the present study, flood mapping depends on AHP as it has many advantages (Kayastha *et al*., 2013); the decision basis is depending on the knowledge of the researchers, every factor can be weighted according to its importance through matrix correlation as shown in Table 5. The limitation of this model is the accurate calculation of factors ranking because it varies from one region to another according to availability of data and the number and importance of each factor.

RESULTS AND DISCUSSION

Land use and land cover (LULC)

Landsat classification means getting equivalent points associated with clusters of homogeneous properties, with the same purpose of selective multiple substances from each other within the image (Elkhrachy, 2015). Before making LULC, points were chosen according to a field survey using Global Positioning System (GPS). The fields survey besides spectral signature of every object using remote sensing are helping us greatly in the confirmation classification, accordingly to that the supervised classification generates eight main LULC for all images, which were classified as transportation facilities, bare lands, urban, irrigated agriculture lands, rain agriculture lands, water bodies, forest lands, and agriculture lands. Data of LULC is very important as a base of food security monitoring in the region of natural hazard. The results adequately explained the large changes and possible interactions between different classes, which indicated that an obvious effect of Khartoum State of climate variables and human use. The percentage of areas of LULC is in the following sequence Agriculture lands > Grasslands > urban lands > Water bodies > Woodlands > Bare lands > Transportation lands > Irrigated agriculture lands. Agriculture lands occupy the largest area with percentage of 37.7 % from the present study area, on the other hand, irrigated agriculture lands occupies about 0.08% of the present study area, as shown in Table 6. Hassaballah *et al*. (2017) said that Woodland removal implies less infiltration due to a gradual decrease in soil permeability, less successful interception of rainfall. According to LULC of the study area, agricultural lands are in danger in any time of flood occurrence causing economic loss of annual production.

Flood susceptibility map

DEM is the most significant factor of hydrological modeling for mapping the hazard index of the flash flood in the study area. Spatial maps are depending mainly on SRTM DEM as watershed and slope, on the other hand, independent factors as surface roughness and LULC for hazard mapping. Flood hazard mapping can be assessed according to elevation data of the study area using ArcGIS. According to DEM, flow direction, flow accumulation, surface roughness, slope and LULC, susceptibility Index was produced to the study area as shown in Figs. 4(a) and 4(b). It should be carefully noted that the areas used are the areas at risk from floods as identified by flow direction and flow accumulation of water. The appropriate direction of water flow, in the eight direction pour-point model diagram, you can properly understand which flow direction water travels. This illustration shows how the values are set. The purple pink is the common color “n” this maps that represents land that slopes to the west (value 16 from our chart above). Therefore, from flow direction, we can detect the vulnerable areas that may be damaged by flash floods. From the present study, it was showed that it may be directed to the low land area. Perhaps more importantly,

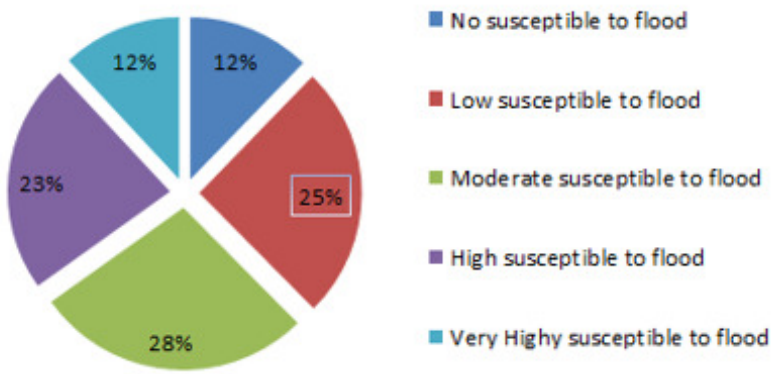

Fig. 5: Flood Susceptibility Index according to ecological factors.

Fig. 6: Photographic image of flood hazards during field survey of the study area

Table 7: Flood Susceptibility Index (FSI)

FSI	Area (Km^2)	Percentage (%)
No susceptible to flood	75.56176	12.26
Low susceptible to flood	156.1465	25.33
Moderate susceptible to flood	169.8991	27.56
High susceptible to flood	141.4005	22.94
Very highly susceptible to flood	73.50499	11.92

a watershed gives diction makers data and supporting items for any sustainable development in the specific area. Accumulation of flow water occurs as a result of excessive rain causing more damage to construction lands. The continuous flow and possible accumulation positively stimulus the water runoff into a single regression association. The slope is typically denoted as a percentage, an angle, or a ratio. The common values of the slope were in the range from zero to 2.37°. When the slope of earth is low, the probability of flooding is high causing damage (Rahmati *et al*., 2016)**.** In the present study, SR ranged from 0 to one. The higher, the more roughness the less susceptibility to flooding. Majority of the study area may be undergone the higher value near to one. Das (2019) said that curvature, rainfall and flow accumulation are not vital in flood mapping. Fig. 5 illustrates the spatial flood susceptibility index and the percentage (%) of susceptibility to flooding. Results indicated that 75.56176 Km^2 (12.26%) of the flooded areas are classified as no susceptible to flood, 156.1465 Km^2 (25.33%) are classified as low susceptible to flooding, about 169.8991 Km^2 (27.56%) are classified flood, 141.4005 Km^2 (22.94%) are classified as very highly susceptible to flood and 73.50499 Km^2 (as moderately susceptible to 11.92 %) are classified as very highly susceptible to flood as shown in Fig. 5 and Table 7. Urban area, vegetation, and woodlands can be affected negatively by flood hazard. Vulnerable areas can cause high destruction of the social and economic network and lead to the loss of human life. Majority of the high susceptibility area to flooding concentrated in the northern part of the study area where the grassland occupies these areas. The vulnerable area called catchments that water and surface run-off will accumulate which will serve as reservoirs for water. For example, roads and railway embankments can be estimated as the main features in the floodplain that could be a potential wall to flood plain flow paths. The findings of the study indicate that the flood vulnerable areas in Sudan are situated in the north east part of the study area. Hazard map was applied to avoid many problems from different features in the earth crust as roads and railway (Sun *et al*., 2007). Flash floods of Sudan may because large amount of ecological hazards. The floods besieged the Jili area from three directions as a result of the pressure on the Nile River. Jelly city in Sudan will not remain and resident after flood occurrence as shown in Fig. 6. Generally, flash flood affect negatively on the ecosystem, especially to fertile soil and vegetation cover which loss the annual yield of crops in these regions. Another effect related to human health as a gradual decline of health with increasing of some diseases as malaria and water-borne diseases as well as potential disturbance of ecosystem services. Jelly city, north of Khartoum was hit by torrential floods that swept the area from the east after the demolition of part of the earth barrier around the city. Hereher (2016) recommended that proper sustainable development occurred as a result of suitable management for the prevention and reducing the hazard of natural resources. Finally, it is recommended that a sensitivity analysis should be carried out before and after flooding to protect the human being and prevent more disasters.

CONCLUSION

The present study presented an efficient model to estimate the flood hazard in Khartoum area, Sudan. The successful integration of satellite data and local products typically derived from the digital model of the ground has allowed the continuous mapping of areas at the considerable hazard of flooding in the Khartoum area, Sudan. The specific application of remote sensing and GIS data generously offered an effective opportunity for changes detection and mapping of LU/LC in the Khartoum State as well as

in arid and semi-arid lands at a moderately cost-effective. APH give an accurate method for mapping the flood sensitivity in the study area. Based on DEM (SRTM), slope, surface roughness, flow accumulation, stream power index, topographic wetness index and curvature of the topography; five classes of flood hazard were applied. Results indicated that 75.56176 Km^2 (12.26%) of the flooded areas are classified as no susceptible to flood, 156.1465 Km^2 (25.33%) are classified as low susceptible to flood, 169.8991 Km^2 (27.56%) are classified flood, 141.4005 Km^2 (22.94%) are classified as very highly susceptible to flood and 73.50499 Km^2 (as moderately susceptible to 11.92 %) are classified as very highly susceptible to flood. Majority of the high susceptibility to flooding concentrated in the northern part of the study area where the grassland occupies these areas. Flash Floods can affect negatively on the environment causing more damage to vegetation cover and construction lands which loss the annual yield of crops in these regions. Finally, the damage of flash flood in Sudan may be reached to human health causing some diseases as malaria and others. Remote sensing and GIS are a precisely accurate and low-cost technique for accurate estimation of flood hazards. Therefore, the present study showed a model of flood sensitivity that can be used an important tool for engineers, governmental institutions and researcher. It is recommended to apply this model in the area with the same climate.

ACKNOWLEDGEMENTS

The authors acknowledge that this study was co-financed by the China-Arab States Technology Exchange Transfer Centre project “Demonstration Study on Multi-Source Remote Sensing Data Monitoring in Flood Inundation in the Nile Region under Grant” [No. 2017EZ10].

CONFLICT OF INTEREST

The author declares that there is no conflict of interests regarding the publication of this manuscript. In addition, the ethical issues, including plagiarism, informed consent, misconduct, data fabrication and/or falsification, double publication and/or submission, and redundancy have been completely observed by the authors.

ABBREVIATIONS

%	Percentage
°C	*Celsius degree*
AHP	Analytical hierarchy process
CI	consistency index
CR	consistency ratio
CT	Curvature Topographic
DEM	Digital Elevation Model
Dd	Drainage density
EM-DAT	Emergency events database
FHI	flood hazard index
Eq	Equation
E	East
Fig	Figure
GF	Gaofen
GIS	Geographic Information system
GPS	Global Positioning System
Km^2	Kilometer
LULC	Land use and land Cover
m	*Meter*
max	*Maximum*
min	*Minimum*
mm	*Millimeter*
N	*North*
PMS	*particulate matter* sensor
RI	random index
SR	Surface roughness
SPI	Stream power index
SRTM	Shuttle Radar Topography Mission
TWI	Topographic wetness index
WFV	wide field view

REFERENCES

Abd El-Hamid, H.T.; Hegazy, T.A.; Ibrahim, M.S.; El-Moselhy, K.M., (2016). Assessment of heavy metals pollution in marine sediments along the Mediterranean Sea, Egypt. J. Geogr. Environ. Earth Sci. Int., 7(4): 1-11 **(11 pages)**.

Abdel Kareem, O.; Khalifa, K.S .O. Adam, H.; Elhaja, M.; Eltahir, M. (2017). Land use land cover changes detection in White Nile State, Sudan using remote sensing and GIS techniques. Int. J. Environ. Monit. Protect., 4(3): 14-19 **(6 pages).**

Abdulrazzak, M.; Elfeki, A.; Kamis, A.; Kassab, M.; Alamri, N.; Chaabani, A.; and Noor, K., (2019). Flash flood risk assessment in urban arid environment: case study of Taibah and Islamic universities’ ampuses, Medina, Kingdom of Saudi Arabia. J.

Geomatics Nat. Hazards Risk. 780-796 **(17 pages).**

Adinarayana, J.; Krishna, N.R., (1996). Integration of multi-seasonal remotely-sensed images for improved land use classification of a hilly watershed using geographical information systems. Int. J. Remote Sens., 17(9): 1679–1688 **(10 pages).**

Anon, (2018). International Research Institute for Climate Society – Climate forcast methodology. International Research Institute.

Beven, K.J.; Kirkby, M.J., (1979). A physically-based variable contributing area model of basin hydrology. Hydrol. Sci. Bull., 24(1): 43–69 **(27 pages).**

Cao, C.; Xu, P.; Wang, Y.; Chen, J.; Zheng, L; Niu, C., (2016). Flash flood hazard susceptibility mapping using frequency ratio and statistical index methods in coalmine subsidence areas. Sustainability 8 (9): 1-18 **(18 pages).**

Chen, P.; Liew, S.C.; Lim, H., (1999). Flood detection using multi temporal radarsat and ERS SAR data, In: Proc. 20th Asian Conference on Remote Sensing, Hong Kong, 22–25.

Chi, Z.X.; Long, X.J.; Du, Z.J.; Sun, X.; Hu, Q.L.; Long, Y., (2019). Climatic experiment on Guizhou red heart Kiwifruit Ulcer Disease. J. Goesci. Environ. Protect., 7: 251-273 **(23 pages).**

Coulibaly, M. (2008). Spatial analysis of an urban flash flood results. Geocar. Int., 23(3): 217–234 **(18 pages).**

Das, S., (2019). Geospatial mapping of flood susceptibility and hydro-geomorphic response to the floods in Ulhas basin, India. Rem. Sens. Applica. Soc. Environ., 14(1): 60–74 **(15 pages).**

Dolman, A.J.; Gash, J.H.C.; Goutorbe, J.P.; Kerr, Y.; Lebel, T.; Prince, S.D.; Stricker, J.N.M., (1997). The role of the land surface in sahelian climate. HAPEX-Sahel results and future research needs. J. Hydrol. 188(189): 1067–1079 **(13 pages).**

Elkhrachy, I., (2015). Flash flood hazard mapping using satellite images and GIS tools: A case study of Najran City, Kingdom of Saudi Arabia (KSA). Egypt. J. Remote Sens. Space Sci., 18: 261–278 **(17 pages).**

EM-DAT, (2018). Centre for Research on the Epidemiology of Disasters (CRED). EM-DAT Database.

Forkuo, E.K., (2010). Digital elevation modeling using aster stereo imagery, J. Environ. Sci. Eng., 52(2): 81-92 **(11 pages).**

Hapuarachchi, H.A.P.; Wang, Q.J.; Pagano, T.C., (2011). A review of advances in flash flood forecasting. Hydrol. Process. 25: 2771–2784 **(14 pages).**

Harun, N.A.; Makhtar, M., Aziz, A. A.; Zakaria, Z .A; Abdullah, F.S.; Jusoh, J.A., (2017). The application of apriority algorithm in predicting flood areas. Int. J. Adv. Sci. Eng. Inf. Technol., 7: 763–769 **(7 pages).**

Hassaballah, Kh. Mohamed, Y., Uhlenbrook, S.; Biro, Kh., (2017). Analysis of stream flow response to land use and land cover changes using satellite data and hydrological modeling: case study of Dinder and Rahad tributaries of the Blue Nile (Ethiopia–Sudan). Hydrol. Earth Syst. Sci., 21: 5217–5242 **(26 pages).**

Hereher, M. (2016). Vulnerability assessment of the Saudi Arabian Red Sea coast to climate change. J. Environ. Earth Sci., 75(1): 1-13 **(13 pages).**

Horritt, M.S., (2000). Calibration of a two-dimensional finite element flood flow model using satellite radar imagery. J. water Res., 36: 3279–3291 **(13 pages).**

Kayastha, P.; Dhital, M.R.; De Smedt, F., (2013). Application of the analytical hierarchy process (AHP) for landslide susceptibility mapping: a case study from the Tina watershed, West Nepal. Comp. Geosci., 52: 398–408 **(11 pages).**

Kazakis, N.; Kougias, I.; Patsialis, T., (2015). Assessment of flood hazard areas at a regional scale using an index-based approach and analytical hierarchy process: application in Rhodope Evros region, Greece. Sci. Total Environ., 538: 555–563 **(9 pages).**

Kia, M.B.; Pirasteh, S.; Pradhan, B.; Rodzi, M.A.; Sulaiman, W.N.A.; Moradi, A., (2012). An artificial neural network model for flood simulation using GIS: Johor River Basin, Malaysia. Environ. Earth Sci., 67: 251–264 **(14 pages).**

Kowalzig, J., (2008). Climate, poverty, and justice: What the Poznań UN climate conference needs to deliver for a fair and effective global deal. Climate, Poverty, Justice, Oxfam Briefing Paper. 4 (3): 117–148 **(32 pages).**

Kumar, P.K.; Gopinath, G.; Seralathan, P., (2007). Application of remote sensing and GIS for the demarcation of groundwater potential zones of a river basin in Kerala, southwest coast of India. Int. J. Remote Sens. 28 (24): 5583–5601 **(19 pages).**

Mahmoud, S.H.; Gan, T.Y.; (2018). Multi-criteria approach to develop flood susceptibility maps in arid regions of Middle East. J. Clean. Product., 196: 216–229 **(14 pages).**

Mastin, M., (2009). Watershed models for decision support for inflows to potholes reservoir, Washington.

Matthew, M.W.; Adler-Golden, S.M.; Berk, A.; Richtsmeier, S.C.; Levine, R.Y.; Bernstein, L.S.; Acharya, P. K.; Anderson, G.P.; Felde, G.W.; Hoke, M.P., (2000). Status of atmospheric correction using a mODTRAN4-based algorithm. Spec. Sci. Inc.: Burlington, MA, USA.

Muneerudeen, A., (2017). Urban and landscape design strategies for flood resilience in Chennai City; Qatar University: Doha, Qatar.

NOAA/NWS, (2005). Floods: The Awesome Power. U.S. Department of Commerce, National Weather Service, ARC 4493, NOAA PA 2000467 **(16 pages).**

Rahmati, O.; Pourghasemi, H.R.; Zeinivand, H., (2016). Flood susceptibility mapping using frequency ratio and weights-of-evidence models in the Golastan Province, Iran. J. Geocarto Int., 31(1): 42-70 **(29 pages).**

Saaty, T.L., (1977). A scaling method for priorities in hierarchical structures. J. Math. Psychol. 15: 234–281 **(48 pages).**

Sulieman, H.M.; Elagib, N.A., (2012). Implications of climate, land-use and land-cover changes for pastoralism in eastern Sudan, J. Ari. Environ., 85: 132-141 **(10 pages).**

Sun, Y.E.; Neil, G.; Daniel, W., (2007). Use of GIS in flood risk rapping, National Hydrology Serminar on GIS in Hydrology Applications – Modelling – Data Issues, Tullamore, Ireland, 1-12 **(12 pages).**

Warner, T.T., (2004). Desert meteorology. Edinburgh: Cambridge university press; p. 612.

AUTHOR (S) BIOSKETCHES

Abdel Hamid, H.T., Ph.D., Assistant Professor, Department of Marine Pollution, National Institute of Oceanography and Fisheries, Alexandria, Egypt and Ningxia Institute of Remote Sensing Surveying and Mapping, Yinchuan 750021 China.
Email: *hazem_ecology@yahoo.com*

Wenlong, W., B.Sc., Instructor, Ningxia Institute of Remote Sensing Surveying and Mapping, Yinchuan 750021 China.
Email: *wwlong2008@qq.com*

Qiaomin, L., B.Sc., Instructor, Ningxia Institute of Remote Sensing Surveying and Mapping, Yinchuan 750021 China.
Email: *379853302@qq.com*

HOW TO CITE THIS ARTICLE

Abdel Hamid, H.T.; Wenlong, W.; Qiaomin, L., (2020). Environmental sensitivity of flash flood hazard using geospatial techniques. Global J. Environ. Sci. Manage., 6(1): 31-46.

DOI: 10.22034/gjesm.2020.01.03

url: https://www.gjesm.net/article_36433.html